Acta Scientific Applied Physics

Volume 3 Issue 4 April 2023

Review Article

Effect of Coils Geometry on Dynamic Wireless Power Transfer for Electric Vehicles

Sahar Bareli[1], Lidor Geri[1], Yasha Nikulshin[1], Oren Nahum[2,3], Yuval Hadas[2], Yosef Yeshurun[1], Eyal Yaniv[4] and Shuki Wolfus[1]*

[1]*Department of Physics, Bar-Ilan University, Israel*

[2]*Department of Management, Bar-Ilan University, Israel*

[3]*Economics and Logistics Studies, Faculty of Economics, Ashkelon Academic College, Israel*

[4]*Graduate School of Business Administration, Bar-Ilan University, Israel*

***Corresponding Author:** Shuki Wolfus, Department of Physics, Bar-Ilan University, Israel.

Received: February 15, 2023

Published: March 13, 2023

Abstract

Dynamic Wireless Power Transfer (DWPT) uses transmitting coils embedded in the road for charging the on-board battery of an Electric Vehicle (EV) while driving. The present work describes a method of finding optimal geometric parameters for receiver coils that corresponds to improved energy transfer. Stationary and dynamic scenarios were simulated to investigate the effect of said coils' dimension on the electromagnetic coupling coefficient, k, and the energy transfer efficiency, η. In the stationary scenario, k exhibits a nonmonotonic dependence on the receiver coil dimension, with its peak corresponding to the optimal coil dimension. The dynamic scenario shows oscillations of k and η along the travel path. Both scenarios are analyzed and explained by the spatial distribution of the magnetic field generated by the transmitter coils. A method for selecting the optimal configuration for the dynamic case is suggested. The method relies on the magnetic flux behavior of the transmitter coils, and can be applied to other receiver configurations as well. Finally, we show that the addition of a ferrite plate between the receiver array and the EV chassis is shown to screen the non-ionizing radiation emitted by the transmitter coils and reduce it to well below the allowed standards.

Keywords: Dynamic Wireless Power Transfer; Smart Transportation; Electric Vehicles

Introduction

Dynamic Wireless Power Transfer (DWPT) technology enables the process of charging the on-board battery of an Electric Vehicle (EV) while on the move along its travel path [1-4]. Transmitter coils under the road transmit electromagnetic energy to the receiver coils mounted under the car chassis. Since the process of charging the EV accompanies the car along its travel path, it allows the on-board battery to be minimized in dimensions, capacity and weight when comparing to more 'traditional' energy transfer methods, such as wired energy transfer. The reduced battery carried by the EV leads to dramatic energy savings due to the reduced vehicle weight. It also leads to a significant environmental advantage caused by minimizing CO_2 emissions and other hazardous waste and contaminants [5].

In designing DWPT systems, one must consider the receiver and transmitter coil dimensions, shapes, and alignments, as these factors drastically affect the magnetic flux pickup efficiency of the system. As EVs become more and more popular, improving their charging efficiency and travel range becomes crucial for allowing the technology to further penetrate the transportation market. One way to improve DWPT efficiency is to improve the electromagnetic

coupling by optimizing the geometry, windings and resonance parameters of the transmitting and/or the receiving coils. The present paper suggests a method for analyzing the effect of receiver coil dimensions and geometry on the coupling coefficient, k, which in turn, affects the overall efficiency of the power transfer. We present an example that shows that k has a strong dependence on the dimensions of the coil in a nonmonotonic manner and its optimal value affects the design of the system.

Various types of coil configurations have been previously suggested for WPT ('stationary' wireless charging) and DWPT applications. These differ in shape, size, polarity, and use of magnetic cores. Examples of WPT and DWPT optimizations can be found in previous works [6-10] where a multi-objective simulation approach was taken to address misalignment issues. Railing types were also explored in previous papers, such as the "I-type" module, which describes an "I" shaped rail [11]. The design was implemented in one of OLEV's systems and offered a good spatial magnetic flux coverage at a somewhat limited range. The "S-type" module was implemented in a newer OLEV system, which included an S-shaped power supply rail for better transmitter range [12]. This improved upon its predecessor by allowing the doubling of the vertical distance between the receiver and the transmitter coils, while also reducing stray electric and magnetic fields (EMF) well below the guidelines. A simple array of circular transmitters was also tested in previous works [13,14]. Unipolar and bipolar transmitter and receiver coils were also tested [2,15-17]. Unipolar coils are easier to implement, as their geometry is simple. However, they are outperformed by their bipolar counterparts, since a bipolar configuration confines the flux lines into a more specific region under the receiver coils, increasing the electromagnetic coupling and reducing residual electromagnetic radiation. One of the most effective receiver bipolar configurations is the "double-D" (DD) shape configuration [2], where two rectangular coils are laid side by side to form a "double-window"-like shape and are connected in opposite direction to pick the net sum of two opposing sign magnetic field lines. Still, the DD configuration is very susceptible to misalignments. Clearly, when the EV travels along the transmitter coils track, large variations in the picked-up flux occur, with a point of minimal signal where the DD layout is positioned above one of the transmitter coils. An overlapped DD transmission coil was explored in [18] to offer better coverage of the transmission array thus improve energy transfer efficiency. On the receiver side, the double-D quadrature (DDQ) configuration [2,17], includes an additional single coil mounted above the center of the DD layout. It provides a good solution to DWPT, since it can pick up increased amounts of magnetic flux lines relative to DD configurations of similar size. It is also far less susceptible to misalignments along the travel path, as the Q coil covers the "dead" zones of the DD coils, effectively increasing the flux pickup.

The present paper explores the effect of dimension variations of the receiver 'DD' coils in the DDQ configuration on the electromagnetic coupling and energy transfer efficiency. By using electromagnetic simulations, we have demonstrated that substantial improvement in energy transfer can be obtained in the 'classic' DDQ configuration. We have also shown that the electromagnetic coupling coefficient, k, is a nonmonotonic function of the receiver coil size, reaching a maximum which may help in defining an optimal coil size. The gap between the two 'D' coils in the 'DD' pair is also varied in our simulations, in an effort to support k enhancement. Finally, the variation in k along the travel path is explored, showing a complex size dependence from which one may select the most efficient configuration. Furthermore, our results show that for a preset vertical distance between the transmitter and receiver coils, the receiver size can be used as a design parameter for obtaining optimal energy efficiency. The DDQ configuration explored here serves to demonstrate the method, which may be applied to any coil configuration.

Simulation Method

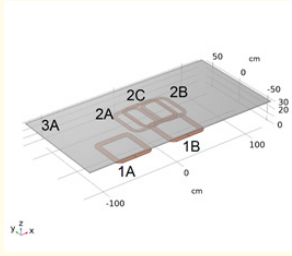

Figure 1: Initial layout of the simulated coil array. 1A, 1B: Transmitter coils. 2A, 2B: DD receiver coils. 2C: Q shaped receiver coil on top of the DD receiver coils. 3A: Ferromagnetic ferrite plate.

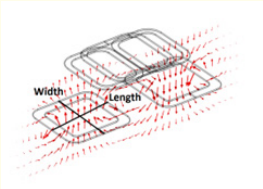

Figure 2: Flux lines generated in the bipolar transmitter coils. Definitions of coil length and width are presented.

The main tool used in our study is numerical simulation. This is to replace a real-life measurement system since every small change to the configuration is costly and slow to produce, therefore impractical. Simulations presented in this work were performed using COMSOL Multiphysics simulation tool [21,22]. The validity of the finite element simulation method and its precision in matching the physical realization of the model has been proven time and again [22].

All simulations were solved using the AC/DC module for COMSOL, specifically using the magnetic field (mf) formulation, which solves the frequency domain Maxwell set of equations for the vector potential A. The frequency domain, rather than the time domain, was chosen, since the time which takes the vehicle to pass over the coils is negligible compared to the frequency of the magnetic field generated by the transmitter coils. Working in the frequency domain drastically improves solving time in this case.

As a starting point in our simulations, we used a DDQ configuration shown in figure 1. Initial values for the coil parameters were obtained from "Electreon Ltd." and are used in typical implementations of DWPT layouts. Each transmitter coil was defined to have 11 turns, while the receiver coils have 3.5 turns each. The transmitter coils form a DD configuration, each coil is 25 cm in width and length (see figure 2 for clarification), placed 25 cm apart from each other. The transmitter coils are connected in series in a "figure of eight" manner, such that the current in one coil flows clockwise, while the current in the second coil flows counterclockwise. The receiver coils are connected in a similar manner, so that flux in opposite directions crossing each 'D' coil is integrated and contributes to the induced voltage. The transmitter coils therefore create a bipolar flux spatial distribution as seen in figure 2, where the flux which enters one coil exits through the other. A ferrite plate of dimensions 250x125x1cm^3 has been placed on top of the receiver coil array. The plate serves to divert flux lines into the receiver coils, as shown in figure 2.

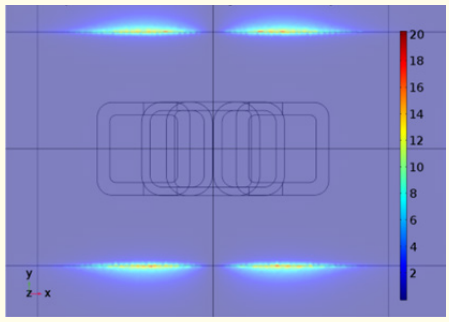

Figure 3: Magnetic induction intensity (mG) at the ferrite plate level.

It also serves as a magnetic shield for reducing electromagnetic non-ionizing radiation level at the passenger's height to well below the allowed standards [23], as seen on figure 3. Here, maximal flux levels (~20 mG) are observed at the edges of the ferrite plate where flux lines exit the plate. Although the non-ionizing radiation levels described here are low enough, it may be further reduced, if required, by varying the design of the ferrite plate.

Variations in the receiver and transmitter coil have been made to both its width and length, with the resulting coils being of rectangular shapes. These changes were made with the goal of collecting more flux lines at the receiving coils, and were proven to be very successful, as described in the next section. In all simulations for the transmitter coils, a 50 A RMS, 85 kHz sinewave current was generated, using frequency domain simulations. Again, these values were selected to correspond with typical 'real-life' implementations.

Results and Discussion

The electromagnetic coupling coefficient of two inductors is given by $k = \frac{L_{1,2}}{\sqrt{L_1 L_2}}$, where L_1 and L_2 are the self-inductances of the transmitter and receiver coils, respectively. The self-inductances are directly correlated with the geometric properties of the coils. $L_{1,2}$ is the mutual inductance between the receiver and transmitter coils $L_{1,2} = V_2 / \frac{di_1}{dt}$ where V_2 is the voltage across the receiver coils, and i_1 is the current in the transmitter coils.

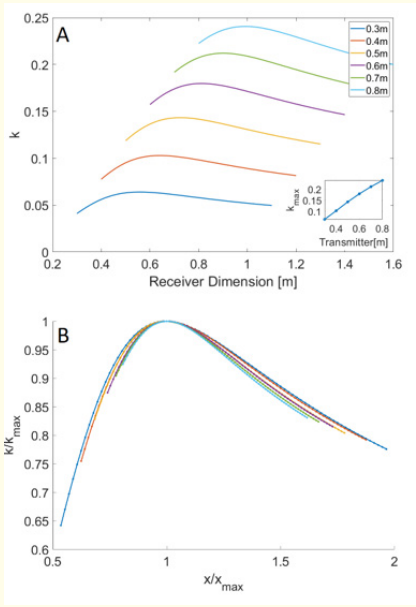

Figure 4: A: The coupling coefficient between the transmitter and the DD coils as a function DD coil length (x). Each curve represents a different transmitter coil dimension from 0.3 to 0.8 m. Inset – transmitter dimension k_{max} dependence. B: k curves normalized by k_{max} and x_{max}.

Figure 4 displays the first set of simulations which explore configurations similar to the base configuration seen in figure 1. Each line in figure 4 represents coils layout with different transmitter coils. The x axis represents the length of the 'DD' receiver coils (the dimension parallel to the axis of advancement). In each simulation step, the length was either stretched or compressed. The width of the receiver was kept fixed at 0.5 m, as the vehicle's width has a tighter dimension restriction than its length. The coupling coefficient, k, increases with the increase in the receiver coil size, in a nonmonotonic manner. For each transmitter size, there is a corresponding receiver size that receives a maximal k value, k_{max}. Beyond this point k decreases with a further increase in receiver size.

The bottom inset in figure 4A displays the dependence of k_{max} on the transmitter coil width and length. k_{max} grows monotonically with the increase in transmitter size exhibiting somewhat weaker than linear dependence.

Using the values of k_{max} and its corresponding dimension, x_{max}, we have scaled each k curve by these values so that each curve's peak falls at $\frac{x}{x_{max}} = 1, \frac{k}{k_{max}} = 1.$. The result of this scaling operation is displayed in figure 4B, showing a nice 'collapse' of the curves into a "universal curve", meaning our method is applicable to any transmitter size.

The explanation to the increase in k with increasing transmitter coil size is trivial. Since the coupling is proportional to the ratio r/h, (h being the vertical distance between coils and r its typical dimension) [1], increasing the size of the transmitter coils is equivalent to reducing the distance between the transmitter and receiver coils. The scaling seen in figure 4B suggests that the increase in transmitter length does not fundamentally change the overall behavior of k,

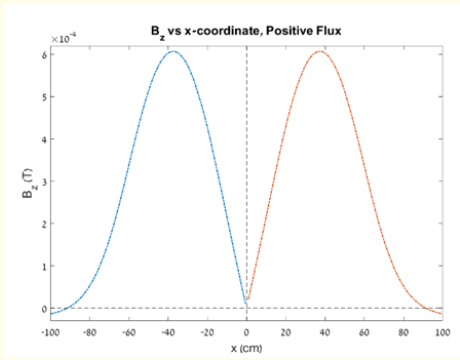

Figure 5: Position dependent B_z along the x-axis. The colors represent a different flux direction. x=0: center of transmitter coil array.

but rather just scales it.

To explain the nonmonotonic behavior of k for each selected transmitter size, one must look at the magnetic field distribution in the XY plane, i.e., the plane of the EV's chassis. Figure 5 describes the z component of the magnetic field (B_z) in the XY plane of the receiver coils, for the 0.5 m sized transmitters. reaches its absolute value maximum at about x = 38 cm / -38 cm respectively. Once we venture past these points, starts diminishing. At around ±90 cm, the field reverses its sign and, therefore, the induced voltage on each receiver coil declines. This, again, can be applied to various sizes of transmitter coil and is not limited to this specific example. The spatial magnetic flux distribution is a key to designing optimal receiver dimensions.

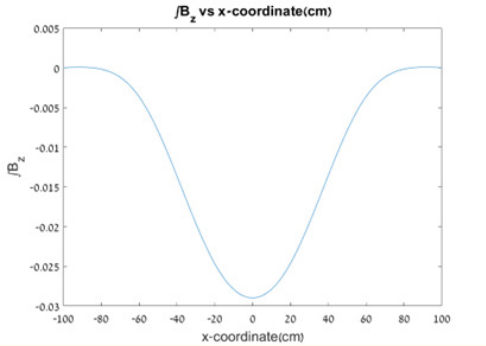

Figure 6: Integrated z component of the magnetic flux density along the x-axis. x=0: center of transmitter coil array.

Figure 6 represents the integral of over the entire x axis:

$$\int_{-100}^{100} B_z(x)dx$$

This correlates well with figures 3 and 4, as the overall flux starts plateauing rapidly at around 0.7 m. This is the point where the flux in figure 5 decreases rapidly and is about to flip and become negative, therefore obstructing further net flux collection. Also, in figure 4 we see that k starts decreasing rapidly after that point, strengthening the claim that once we go past this point, flux collection becomes less significant.

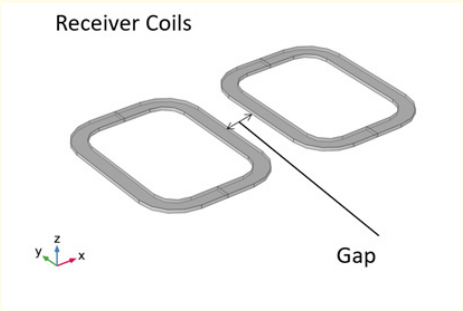

Figure 7: Added gap between the 'DD' coils.

By analyzing the flux distribution, we can gather from figures 5 and 6 that the flux collection is minimal around the center (X = 0), implying that it can be potentially more effective to separate the DD configuration and add a gap between the two "D" coils, as seen in figure 7.

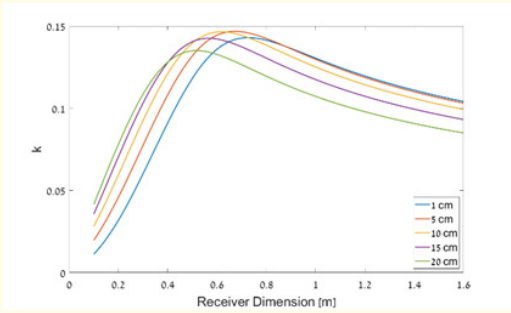

Figure 8: Comparison between different separating gaps.

Figure 8 describes the changes in k for different separations for the case of the default 38 cm 'D' "radius". Each line represents a different distance between the D-shaped coils. For small receiver coil dimensions, we clearly see that k increases with increasing separation. For example, for receiver coils of 0.3 m, k increases from about 0.05 for 1 cm separation to ~0.12 for 20 cm distance, nearly a 3-fold improvement. This is attributed to the expected increased flux collection as we center the "D" coil around the maxima in B_z. However, for large coils, we see a reversal of this behavior and k of smaller separation distance is higher than k of larger distances. Again, we can explain the results as the horizontal shift of the coil brings larger coils into the reversed flux region hence decreases k. For the sake of the example presented in this paper, a separation of 10 cm is chosen for the case of 38 cm receiver coils. For these separation intervals, k reaches the highest level, while also being more cost efficient than just changing the dimensions of the coils. Putting it all together, we can get an ideal 'DDQ' – type of configuration for

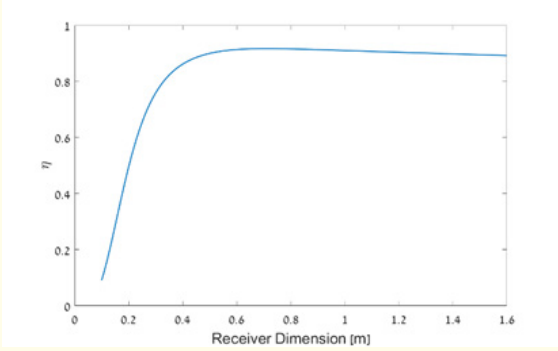

Figure 9: Energy transfer efficiency for the 10 cm separation case.

our receiver coils that are best suited for a static case. These results are next carried over to the dynamic phase of the simulations.

The maximal efficiency of an inductively coupled resonator system is given by [4]:

$$\eta_{opt} = \frac{k^2 Q_1 Q_2}{\left(1+\sqrt{1+k^2 Q_1 Q_2}\right)^2}$$

Where Q_1,Q_2 are the quality factors of the transmitter and receiver circuits, respectively. In our study case, Q_1 and Q_2 are calculated to be 52.3 and 467.7 respectively. Note that a series resistance was added to the transmitter coils, therefore reducing . Assuming a value of 0.15 for k, which is the maximal value of k we have reached in the static simulations for a 0.5 m transmitter (figures 4 and 8), one can get a maximal efficiency of:

$$\eta_{opt} \approx 0.92$$

Figure 9 describes the changes in the efficiency as a function of the receiver coil size. The efficiency increases steeply from about 10% for coils of 10 cm radius to about 90% for coils of about 60 cm size. A further increase in the receiver size results in a slowly declining efficiency. Therefore, for the practical case, by increasing the receiver coils size from 38 cm to 60 cm, we managed to increase the efficiency of the system from about 80% to almost 92%, simply by applying our flux observational method.

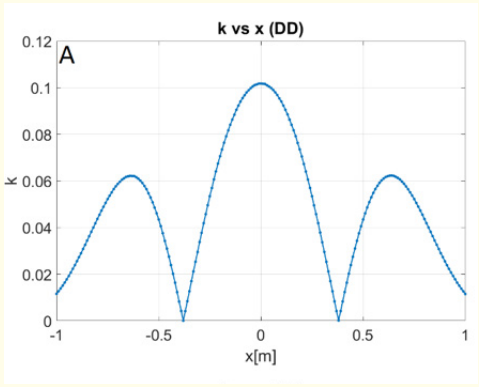

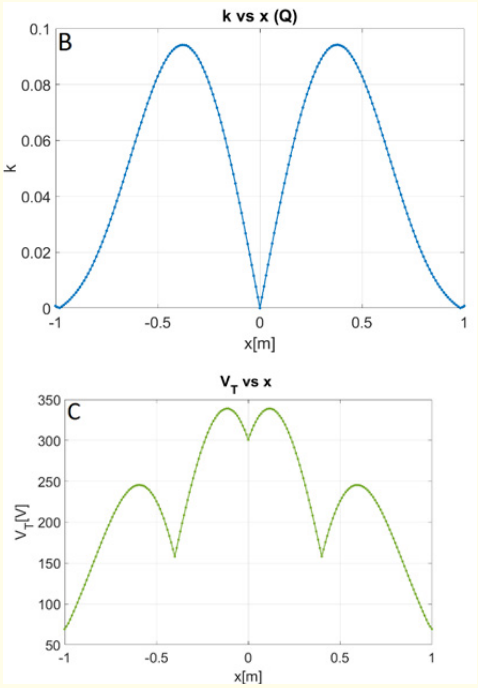

Figure 10: Changes to k at different x-axis positions. A: Coupling coefficient between transmitters and DD coils. B: Coupling coefficient between transmitters and Q coil. C: Total induced voltage across combined receiver coils (DDQ). x=0: center of transmitter coil array.

Dynamic Results

The previous sections described an example of a one-dimensional optimization study for increasing the coupling coefficient, and the energy transfer efficiency in stationary states. However, the EV and its receiver coils array travel along its route and the relative distance between the transmitter and receiver coils changes with the EV movement. Variations in the relative positions of both set of coils might occur in all 3-dimentions. Not only that the EV changes its position along its travel line (x-axis movement), but transverse deviations from the charging path occur as well and are inevitable.

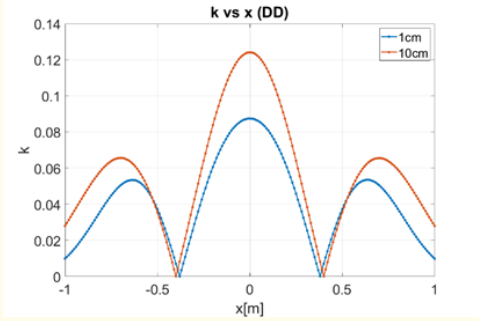

Figure 11: Changes in k (DD) at different x-axis positions for two DD coils spacing: the default 1 cm case, and the 10 cm case. x=0: center of transmitter coil array.

The changes in k along the travel path of an EV can be seen in figure 10, which describes the movement of a 0.4 m wide receiver array along the x-axis. The 'Q' coil is mounted at the center of the receiver coils array so that its coupling coefficient peaks (fig. 10B) where the coupling of the 'DD' is minimal (fig. 10A). Hence, the 'DDQ' configuration proves to have a good flux collection coverage. Since coupling coefficients of the DD and Q coils are not simply additive, figure 10.C shows the sum of the voltage induced in the DD and Q coils. The induced voltage is indeed smoother than k and never reaches zero, however, strong variations in k during a pass

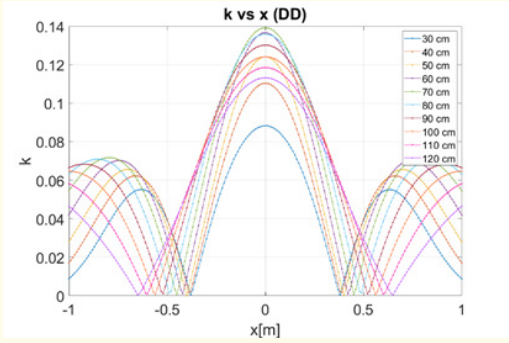

Figure 12: Position dependence of k in DD coils for different coil sizes. x=0: center of transmitter coil array.

over the receiver coils array are evident and still strongly affect the induced volage. This dynamic nature of k must be taken into account on our proposed method.

Figure 11 demonstrates how the 10 cm spacing case (red curve in the figure) is superior in almost every way to the default 1 cm spacing case (blue curve). Throughout the entire path, k (DD) for the 10 cm spacing remains mostly higher than k for the 1 cm case, while also increasing by over 20% in the middle of the path. This, again, is consistent with the magnetic field distribution shown in figures 5 and 6. More flux can be collected if we place the 'DD' coils away from the center. Spacing the receiver coils away from each other is therefore the conclusion which emerges from both stationary and dynamic position scenarios.

Next, we extended the stretching simulations presented in the previous section to the dynamic system. The results are presented in figure 12. Each line represents a different DD coils size, ranging from 30 cm to 120 cm, and the variations in k along the travel path. Clearly, k changes significantly as we move along the travel path,

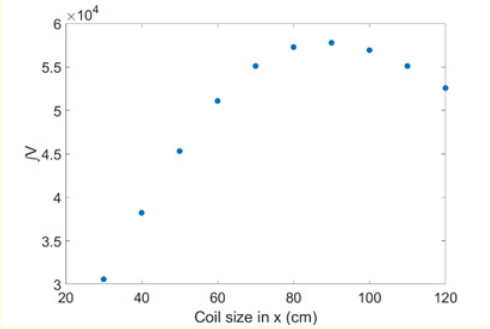

Figure 13: Total (integrated) voltage as a function of the receiver coil size.

and one cannot select straight forward the optimal DD dimension since many of the curve's present a "winning" k values in some positions along the path and "losing" in others. Similar to the stationary scenario presented in figure 5, the peaks in k occur where the receiver coils largely encapsulate the magnetic flux generated by the transmitters. The largest peak in k occurs at the 70 cm case with an impressive 0.14 value at the center of the system, which corresponds to the previous stationary results presented in figures 4 and 8. Another feature seen in the figure is the widening of the k curve with the increase in DD coils dimension. For larger coils, the collected flux is smaller than the 70 cm case but spread-out more evenly throughout space. It is therefore rather difficult to determine which coil configuration is optimal throughout a continuous drive across the transmitter array.

Since an optimal DD length cannot be selected intuitively, we suggest an integration of the total induced voltage for each case. Figure 13 presents the values for the integrated induced voltage, including the induced voltage in the Q coil. We can therefore get the total induced flux in the DDQ coils for each curve presented in figure 12. We note that direct integration of k carries no physical meaning, hence the voltage integration, which is related to the total energy picked up by the coils during a full transition over the transmitter array. In the specific case study, we have presented throughout the paper, the optimal size for the 'DD' coils appears to be between 80-100 cm. Results such as these are very important for our understanding of DWPT, as it accounts for dynamic changes to the system parameters while in motion. Such results provide a method for finding a clear, optimal working point for the dimensions of 'DDQ' configurations. For more practical uses, one can extend the resolution of the simulation and find a more accurate maximal point.

Conclusions

In this paper we have presented a method for analyzing and producing optimal receiver dimensions for DWPT systems. The DDQ coil configuration served as an example study that demonstrated how various changes to the classic DDQ configuration in the receiver coils can greatly affect the coupling coefficient between the receiver and transmitter systems. This results in a better and more efficient energy transfer. Using our method, we were able to find an optimal length to our receiver coils and an optimal spacing between them.

In our case study, we found that the coupling coefficient increases with increasing receiver size, peaks at an optimal size and decreases thereafter. These findings were explained by analyzing the spatial distribution of the magnetic field, which shows that the net magnetic flux crossing the receiver coils starts to decrease above the optimal dimension due to magnetic field direction reversal. We have also examined the proposed changes and tweaks made in the stationary case under a drive scenario when the EV travels along the transmitter coils segment. It was shown that the optimized stationary configuration is not the optimal configuration for the

Bibliography

1. Y Gao., *et al*. "Misalignment effect on efficiency of wireless power transfer for electric vehicles". in 2016 IEEE Applied Power Electronics Conference and Exposition (APEC), (2016): 3526-3528.

2. C C Mi., *et al*. "Modern advances in wireless power transfer systems for roadway powered electric vehicles". *IEEE Transactions on Industrial Electronics* 63.10 (2016): 6533-6545.

3. S Y Choi., *et al*. "Advances in wireless power transfer systems for roadway-powered electric vehicles". *IEEE Journal of Emerging and Selected Topics in Power Electronics* 3.1 (2014): 18-36.

4. Z Zhang., *et al*. "Wireless power transfer—An overview". *IEEE Transactions on Industrial Electronics* 66.2 (2018): 1044-1058.

5. Shimizu., *et al*. "Potential for CO2 Reduction by Dynamic Wireless Power Transfer for Passenger Vehicles in Japan". *Energies* 13.13 (2020): 3342.

6. S Lee., *et al*. "On-line electric vehicle using inductive power transfer system". in 2010 IEEE Energy Conversion Congress and Exposition (2010): 1598-1601.

7. Y D Ko and Y J Jang. "The optimal system design of the online electric vehicle utilizing wireless power transmission technology". *IEEE Transactions on Intelligent Transportation Systems* 14.3 (2013): 1255-1265.

8. N P Suh., *et al*. "Design of on-line electric vehicle (OLEV)". in Global product development, Springer, (2011): 3-8.

9. R Bosshard and J W Kolar. "Multi-objective optimization of 50 kW/85 kHz IPT system for public transport". *IEEE Journal of Emerging and Selected Topics in Power Electronics* 4.4 (2016): 1370-1382.

10. W Shi., *et al*. "Design of a Highly Efficient 20 kW Inductive Power Transfer System with Improved Misalignment Performance". *IEEE Transactions on Transportation Electrification* (2021).

11. J Huh., *et al*. "Narrow-width inductive power transfer system for online electrical vehicles". *IEEE Transactions on Power Electronics* 26.12 (2011): 3666-3679.

12. S Y Choi., *et al*. "Ultraslim S-type power supply rails for roadway-powered electric vehicles". *IEEE Transactions on Power Electronics* 30.11 (2015): 6456-6468.

13. J M Miller., *et al*. "Demonstrating dynamic wireless charging of an electric vehicle: The benefit of electrochemical capacitor smoothing". *IEEE Power Electronics Magazine* 1.1 (2014): 12-24.

14. X Zhang., *et al*. "Coil design and efficiency analysis for dynamic wireless charging system for electric vehicles". *IEEE Transactions on Magnetics* 52.7 (2016): 1-4.

15. GA Covic., *et al*. "A three-phase inductive power transfer system for roadway-powered vehicles". *IEEE Transactions on Industrial Electronics* 54.6 (2007): 3370-3378.

16. G A Covic and J T Boys. "Inductive power transfer". *Proceedings of the IEEE* 101.6 (2013): 1276-1289.

17. M Budhia., *et al*. "Magnetic design of a three-phase inductive power transfer system for roadway powered electric vehicles". in 2010 IEEE Vehicle Power and Propulsion Conference (2010): 1-6.

18. Y Liu., *et al*. "Efficiency optimization for wireless dynamic charging system with overlapped DD coil arrays". *IEEE Transactions on Power Electronics* 33.4 (2017): 2832-2846.

19. GA Covic and JT Boys. "Modern trends in inductive power transfer for transportation applications". *IEEE Journal of Emerging and Selected Topics in Power Electronics* 1.1 (2013): 28-41.

20. C Multiphysics. "Introduction to comsol multiphysics®". COMSOL Multiphysics, Burlington, MA, accessed Feb 9 (2018): 1998.

21. C Zienkiewicz., *et al*. "The finite element method: its basis and fundamentals". Elsevier, (2005).

22. B Szabó and I Babuška. "Finite Element Analysis: Method, Verification and Validation". (2021).

23. J Lin., *et al*. "ICNIRP Guidelines for limiting exposure to time-varying electric and magnetic fields (1 Hz to 100 kHz)". *Health Physics* 99 (2010): 818-836.